Molecular Neurobiology (2019) 56:2978–2989
https://doi.org/10.1007/s12035-018-1279-2

Synthetic Prion Selection and Adaptation

Edoardo Bistaffa[1,2] · Fabio Moda[2] · Tommaso Virgilio[2,3] · Ilaria Campagnani[2] · Chiara Maria Giulia De Luca[2] · Martina Rossi[1] · Giulia Salzano[1] · Giorgio Giaccone[2] · Fabrizio Tagliavini[2] · Giuseppe Legname[1,4]

Received: 4 April 2018 / Accepted: 23 July 2018 / Published online: 3 August 2018

Abstract

Prion pathologies are characterized by the conformational conversion of the cellular prion protein (PrP^{C}) into a pathological infectious isoform, known as PrP^{Sc}. The latter acquires different abnormal conformations, which are associated with specific pathological phenotypes. Recent evidence suggests that prions adapt their conformation to changes in the context of replication. This phenomenon is known as either prion selection or adaptation, where distinct conformations of PrP^{Sc} with higher propensity to propagate in the new environment prevail over the others. Here, we show that a synthetically generated prion isolate, previously subjected to protein misfolding cyclic amplification (PMCA) and then injected in animals, is able to change its biochemical and biophysical properties according to the context of replication. In particular, in second transmission passage in vivo, two different prion isolates were found: one characterized by a predominance of the monoglycosylated band (PrP^{Sc}-M) and the other characterized by a predominance of the diglycosylated one (PrP^{Sc}-D). Neuropathological, biochemical, and biophysical assays confirmed that these PrP^{Sc} possess distinctive characteristics. Finally, PMCA analysis of PrP^{Sc}-M and PrP^{Sc}-D generated PrP^{Sc} (PrP^{Sc}-PMCA) whose biophysical properties were different from those of both inocula, suggesting that PMCA selectively amplified a third PrP^{Sc} isolate. Taken together, these results indicate that the context of replication plays a pivotal role in either prion selection or adaptation. By exploiting the ability of PMCA to mimic the process of prion replication in vitro, it might be possible to assess how changes in the replication environment influence the phenomenon of prion selection and adaptation.

Keywords Synthetic prion · Prion · Adaptation · Selection · PMCA · RT-QuIC

Edoardo Bistaffa and Fabio Moda contributed equally to this work.

Electronic supplementary material The online version of this article (https://doi.org/10.1007/s12035-018-1279-2) contains supplementary material, which is available to authorized users.

✉ Giuseppe Legname
legname@sissa.it

Edoardo Bistaffa
ebistaffa@sissa.it

Fabio Moda
Fabio.moda@istituto-besta.it

Tommaso Virgilio
tommaso.virgilio@irb.usi.ch

Ilaria Campagnani
ilarialaveterinaria@libero.it

Chiara Maria Giulia De Luca
chiara.deluca@istituto-besta.it

Martina Rossi
martina.rossi@sissa.it

Giulia Salzano
gsalzano@sissa.it

Giorgio Giaccone
giorgio.giaccone@istituto-besta.it

Fabrizio Tagliavini
fabrizio.tagliavini@istituto-besta.it

[1] Laboratory of Prion Biology, Department of Neuroscience, Scuola Internazionale Superiore di Studi Avanzati (SISSA), Trieste, Italy

[2] Unit of Neuropathology and Neurology 5, Fondazione IRCCS Istituto Neurologico Carlo Besta, Milan, Italy

[3] Present address: Institute for Research in Biomedicine, Università della Svizzera Italiana, Bellinzona, Switzerland

[4] ELETTRA Laboratory, Sincrotrone Trieste S.C.p.A, Basovizza, Trieste, Italy

Introduction

Prions are pathological agents responsible for a variety of infectious and incurable neurodegenerative disorders, named prion diseases or transmissible spongiform encephalopathies (TSEs). These maladies are characterized by the accumulation in the central nervous system (CNS) of misfolded forms of the prion protein (PrP^{Sc}), which derives from conformational conversion of the normal prion protein (PrP^{C}). PrP^{Sc} can recruit and convert normal PrP^{C}, thus spreading throughout the CNS and leading to the host death. Both PrP^{C} and PrP^{Sc} have two N-linked glycosylation sites that determine the formation of unglycosylated, monoglycosylated, and diglycosylated species. Although both proteins have the same amino acid sequence, PrP^{Sc} has a higher content of β-sheet structures, is insoluble in non-ionic detergents and is partially resistant to Proteinase K (PK) digestion [1]. Different conformations of PrP^{Sc} [2] (referred to as "prion strains") are associated with unique clinical, neuropathological, and biochemical alterations [3]. Neuropathologically, a prion strain can be identified on the basis of the following: (i) incubation and survival time [4], (ii) clinical signs (e.g., rough coat, ataxia, loss of weight) [5], (iii) pattern of PrP^{Sc} deposition (e.g., synaptic, peri-neuronal, amyloid plaques) [6], and (iv) degree of vacuolation in specific brain areas which are produced in experimentally infected animals [7]. Biochemically, there are four main characteristics enabling prion strain classification (after PK digestion): (1) the electrophoretical mobility of the unglycosylated band, (2) the glycosylsation profile of PrP (glycoform ratio) [8], (3) the extent of protease digestion [1], and (4) the resistance to denaturation using chaotropic agents (e.g., guanidine hydrochloride) [9]. Using different analytical approaches, including Fourier transform infrared spectroscopy (FTIR), atomic force microscopy (AFM), and circular dichroism (CD), it has been shown that differences in prion strains lie in their different conformations [10, 11]. Compelling evidence suggests that although lacking DNA or RNA, this protein is surprisingly capable of adapting its pathological conformation to a large landscape of environments [12]. For instance, the inoculation of the same prion strain responsible for the transmission mink encephalopathy (TME) in Syrian hamster gave rise to two different prion strains named hyper (HY) and drowsy (DY), according to the behavioral alterations observed in injected animals. A proposed explanation for this phenomenon might be the fact that TME is not a pure strain but is instead composed by at least two pathological PrP^{Sc} conformations and only one prevails in mink [13]. When challenged in Syrian hamsters, two alternative PrP^{Sc} conformations arise: the first one induces severe and rapid neuropathological alterations and hyperactivity in animals (HY) while the second one is associated with slow disease progression and lethargy (DY) [14, 15]. Biochemical and histological analysis of CNS confirmed that these PrP^{Sc} conformations possess different electrophoretical mobility, distinct resistance to PK digestion, stability against guanidine hydrochloride, and induced different neuropathological alterations [11, 16, 17]. This represents the ability of prions to undergo the process of adaptation or selection according to changes in the environment of replication (mink CNS vs hamster CNS). Although this phenomenon is still poorly understood, the advent of synthetic prions generated in vitro from recombinant source of PrP [18, 19] provides a powerful tool for studying different features of prions, including their capability to modifying the conformation in different environments. The use of synthetic prions enables to study these effects in a highly pure system without the interference of other components which are instead present in the brain when studying natural prion. One of the most fascinating aspects of synthetic prions is their ability to behave as the bona fide prions. These experiments showed for the first time that the pathological properties of different PrP^{Sc} are solely enciphered in their abnormal conformations. Not only genetically modified animals but also wild-type animals can be infected by recombinant prions [20–22]. For example, hamsters infected with a synthetic hamster prion strain succumbed to a disease that was named SSLOW (synthetic strain leading to overweight) [22]. We have recently shown that also wild-type mice can be infected with synthetic mouse prion strain produced under specific experimental conditions [23].

These studies were performed using two innovative and ultrasensitive techniques named protein misfolding cyclic amplification (PMCA) and real-time quaking induced conversion (RT-QuIC). PMCA technique, originally developed by Claudio Soto in 2001 [24], is able to reproduce in vitro the phenomenon of prion replication which occurs in vivo but in an accelerated manner. Particularly, PMCA consists in cycles of incubation and sonication of samples that contain trace amount of PrP^{Sc} in the presence of an excess of PrP^{C}. The sonication phase is able to fragment the PrP^{Sc} aggregates in small polymers which are able to further convert new molecules of PrP^{C} to PrP^{Sc}. Therefore, after several cycles of PMCA, the amount of PrP^{Sc} increases to a level easily detectable with common biochemical assays (e.g., Western blot) [25, 26]. The RT-QuIC [27] technique is based on incubation and subsequent shaking where recombinant soluble prion proteins (recPrP) are induced to aggregate into amyloid structures by the addition of samples that contain trace amount of PrP^{Sc} (referred as "seed"). The aggregation of the recombinant proteins is monitored by Thioflavin T (ThT) fluorescence and enables the detection of amyloid structures in a real time manner.

Recently, PMCA has been used to assess different aspects of prion diseases including the species barrier and the strain adaptation. In the first case, by PMCA experiments, Castilla et al. [28] showed the ability of brain-derived mouse PrP^{Sc} to convert hamster PrP^{C}, thus generating unique prions that were infectious to wild-type hamsters. Other prion strains showed the ability to cross the species barrier using PMCA technique as reported for CWD [29] and for different mouse-adapted prion strains [30]. To study the phenomenon of prion strain

adaptation, PMCA substrate compositions were altered in order to evaluate the biochemical properties of amplified PrP^{Sc}. As reported, changing the RNA content in the substrate of amplification led to the generation of a new prion strain [31]. Particularly, 263K prion strain was adapted to hamster RNA-depleted substrate and then re-adapted to an environment containing RNA. These modifications gave rise to a novel PrP^{Sc} with unique biochemical (conformational stability and replication rate) and infectious characteristics that strongly differ from the original 263K strain. Taken together, these studies provided strong evidence that prions undergo a phenomenon of selection and adaptation when the context of replication is modified [32].

In this work, we describe the ability of a synthetic mouse prion generated from our group [23] to change its biochemical properties when challenged in vivo or in vitro by means of PMCA. In vivo experiments revealed that after serial transmission passages, we were able to identify two distinct conformations of PrP^{Sc}. One of these conformations was characterized by a prevalence of the diglycosylated isoform of PrP^{Sc} (PrP^{Sc}-D) while the other was characterized by the prevalence of the monoglycosylated isoform (PrP^{Sc}-M). Both abnormal conformations were associated with distinct clinical, biochemical, and neuropathological alterations. PMCA analysis of PrP^{Sc}-D and PrP^{Sc}-M revealed that, regardless of the inoculum, the amplified product was characterized by a prevalence of the diglycosylated form of PrP (PrP^{Sc}-PMCA). These data suggest that the synthetic prion we have generated can adapt its conformation according to changes of the context of replication.

Materials and Methods

Ethics Statement

Mice were housed in groups of two to five animals in individually ventilated cages, daily fed and water provided ad libitum. Lighting was on an automatic 12 h basis. Regular veterinary care was daily performed for assessment of animal health. Animal facility is licensed and inspected by the Italian Ministry of Health. Current animal husbandry and housing practices comply with the Council of Europe Convention ETS123 (European Convention for the Protection of Vertebrate Animals used for Experimental and Other Scientific Purposes; Strasbourg, 18.03.1986); with the Italian Legislative Decree 26/2014, Gazzetta Ufficiale della Repubblica Italiana, 26 July 2014; and with the 86/609/EEC (Council Directive of 24 November 1986 on the approximation of laws, regulations, and administrative provisions of the Member States regarding the protection of animals used for experimental and other scientific purposes). The study, including its Ethics aspects, was approved by the Italian Ministry of Health (Permit Number, NP-02–14). The animals were anesthetized with tribromoethanol and all surgery and efforts were made to minimize suffering.

Intracerebral Inoculation

Six-week-old Crl:CD1(ICR) (CD-1) mice (35–40 g) were anesthetized with tribromoethanol (100 μL/10 g) i.p. administered and 2 μl of each brain homogenate collected from the animals of the first passage [23] and prepared in sterile phosphate buffer (10%, weight/volume) was stereotactically injected in the hippocampus. All surgical procedures were performed under sterile conditions. Incubation time (IT) was calculated considering the days between inoculation and symptoms onset including ataxia (uncoordinated movement), tail rigidity, and kyphosis (hunched back). Survival time (ST) was calculated considering the days between the inoculation and the sacrifice of the animals at terminal stages of the disease. Brains were then harvested and half of them were collected for biochemical analysis and the other part was processed for histological evaluations.

Neuropathological Analysis

Brains were fixed in Alcolin (Diapath), dehydrated, and embedded in paraplast. Seven-micrometerthick serial sections were stained with hematoxylin and eosin (H&E), stained with thioflavin S, or immunostained with monoclonal antibodies to PrP (6H4, Prionics), and polyclonal antibodies to glial fibrillary acidic protein (GFAP, Dako). Before PrP immunostaining, the sections were pre-treated with Proteinase K (10 μg/mL, 5 min, room temperature; Invitrogen) and guanidine isothiocyanate (3 M, 20 min, room temperature). Non-specific binding of the antibody was prevented using ARK kit (Dako). Immunoreactions were visualized using 3–3′-diaminobenzidine (DAB, Dako) as chromogen. Lesion profile was performed on H&E-stained sections according to Fraser H. et al. [7]. The areas evaluated were as follows: (1) dorsal medulla, (2) cerebellar cortex, (3) superior culliculus, (4) hypothalamus, (5) thalamus, (6) hippocampus, (7) septum, (8) retrosplenial and adjacent motor cortex, (9) cingulated and adjacent motor cortex. For each area, the severity of vacuolar lesions was graded 0 (no lesions) to 3 (extensive vacuolization) and the mean scores were calculated and then plotted with ± S.E.M. IHC images were acquired at × 10 magnification; H&E images were acquired at × 40 magnification (hippocampus acquired at × 20, dotted box) with a Nikon Eclipse E800 microscope equipped with a Nikon digital camera DXM 1200 and Nikon ACT-1 (v2.63) acquisition software.

Biochemical Analysis

Ten percent (weight/volume) brain homogenates were prepared in lysis buffer (NaCl 100 mM, EDTA 10 mM, NP40 0.5%, Na-deoxycholate 0.5%, Tris-HCl pH 7.4 10 mM). After a brief centrifugation (800×*g*, 1 min), 20 μL of cleared lysate was digested with 50 μg/mL of Proteinase K (1 h, 37 °C, 550 rpm; Invitrogen). PK digestion was stopped by adding loading buffer (sample buffer 4× and DTT 10×, Thermo Scientific) and the samples were boiled (100 °C, 10 min). The proteins were separated using 12% Bis-Tris plus gels (Thermo Scientific) and transferred into polyvinylidene difluoride membranes (PVDF, Millipore). After non-fat dry milk blocking (1 h, room temperature), the membrane was probed using monoclonal anti-PrP 6D11 (0.2 μg/mL; Covance) diluted in TBST and 0.05% Tween-20 (Sigma). After incubation with Fab fragment anti-mouse IgG conjugated with horseradish peroxidase (HRP) (GE), blots were developed using the ECL Prime detection system (Amersham) and chemiluminescence was visualized using a G:BOX Chemi Syngene system.

PMCA Procedures

PMCA was performed as previously described [24]. Briefly, brain homogenate from outbred CD-1 mice prepared in conversion buffer (PBS 1× containing 150 mM sodium chloride and 1% Triton X-100) with the addition of complete protease inhibitor cocktail (Roche) was used as substrate. Ten microliters of brain homogenates from infected mice was added to the substrate and transferred in 0.2-mL PCR tubes, positioned on an adaptor placed on the plate holder of a micro-sonicator (Misonix, Model S3000) and subjected to 96 cycles of PMCA. Each cycle (referred as PMCA round) consisted of 29′ and 40″ sec of incubation at 37/40 °C and 20″ pulse of sonication set at potency of 260–270 W. After one round of PMCA, 10 μl of the amplified material was diluted 10-folds into fresh substrate and a further PMCA rounds were performed. In order to increase the efficiency of amplification, three teflon beads were added to the reaction tube. To prevent samples cross-contamination, all the instruments and equipment were decontaminated using 2 N sodium hydroxide (NaOH; Sigma) or 4 M guanidine hydrochloride (GdnHCl; Sigma) and all the experiments were conducted with appropriate negative control.

PK Resistance Assay

Twenty microliters of brain homogenate or PMCA products was digested with five increasing concentrations of PK enzyme (50, 100, 250, 500, 1000 μg/mL). Samples were then immunoblotted with 6D11 antibody and densitometric analysis of resulting PK-resistant PrP band was performed.

Conformational Stability Assay

Fifty microliters of brain homogenate or PMCA products was incubated with 450 μL of guanidine hydrochloride (GdnHCl) solutions (Sigma) at different molar concentrations (0, 1.5, 3, 4.5, and 6 M) for 2 h at 25° with agitation (550 rpm). Subsequently, an equal volume of Sarkosyl 20% was added to the samples and incubated for 10 min with gentle shaking. Samples were then centrifuged at 100,000×*g* for 1 h at 4 °C. Pellets were washed with equal volume of PBS 1× (Gibco) and then centrifuged at 100,000×*g*, 30′ at 4 °C. The pellets were finally suspended in 50 μL of loading buffer and then processed for Western blot analysis (see the "Biochemical Analysis" section for details). The membrane was incubated with anti-PrP 6D11 primary antibody (0.2 μg/mL; Covance). Densitometric analysis was performed. The concentration of GdnHCl required to unfold half of PrP^{Sc} ($[GdnHCl]_{1/2}$) was then calculated with GrapPad software (v5.0) after non-linear regression curve fit (Boltzmann sigmoidal) of densitometric data.

Recombinant Full-length Mouse PrP Production and Purification

The pET-11a plasmid (Novagen) encoding for the full-length MoPrP(23–231) was kindly provided by Dr. J.R. Requena (University of Santiago de Compostela, Santiago de Compostela, Spain). The mouse construct was expressed in competent BL21 Rosetta2 (DE3) cells *Escherichia coli* (Stratagene). Freshly transformed overnight culture was inoculated into Luria Bertani (LB) medium and 100 μg/mL ampicillin and 30 μg/mL chloramphenicol. At 0.8 OD_{600}, expression was induced with isopropyl b-D galactopyranoside (IPTG) to a final concentration of 1 mM. Cells were grown in a BioStat-B plus fermentor (Sartorius). The cells were lysed by a homogenizer (PandaPLUS 2000) and the inclusion bodies were suspended in buffer containing 25 mM Tris-HCl, 5 mM EDTA, 0.8% TritonX100, and pH 8 and then in bi-distilled water several times. Inclusion bodies containing MoPrP(23–231) were dissolved in 5 volumes of 8 M guanidine hydrochloride (GdnHCl), loaded onto pre-equilibrated HiLoad 26/60 Superdex 200-pg column, and eluted in 25 mM Tris-HCl (pH 8.0), 5 mM ethylenediaminetetraacetic acid, and 5 M GdnHCl at a flow/rate of 1.5 mL/min. Proteins refolding was performed by dialysis against refolding buffer [20 mM sodium acetate and 0.005% NaN_3 (pH 5.5)] using a Spectrapor membrane (molecular weight, 10,000). Purified protein was analyzed by SDS-polyacrylamide gel electrophoresis under reducing conditions and Western blot.

RT-QuIC Analysis

RT-QuIC was performed as previously described with few modifications [33]. Briefly, recombinant full length mouse PrP (23–231) were filtered through a 100 kDa Nanosep centrifugal device (Pall Corporation) and mixed with the reaction buffer composed of the following: 0.2 mg/mL recMoPrP(23–231), 10 mM PBS, 130 mM NaCl, 1 mM EDTA, 0.002% SDS, and 10 μM ThT (all reagents from Sigma). Ninety-eight microliters of the final reaction volume was dispensed in black 96-well optical flat bottom plate (Thermo Scientific). To avoid contaminations, reaction mix was prepared in a prion-free laboratory and all the samples were analyzed in triplicate. After the addition of 2 μL of brain homogenate or PMCA amplified products, the plate was sealed with a sealing film (Thermo Scientific) and inserted into a FLUOstar OPTIMA microplate reader (BMG Labtech). The plate was shaken for 1 min at 600 rpm (double orbital) and incubated for 1 min at 42 °C. A sample was considered positive if two out of three replicates crossed the threshold of 30% of the maximum ThT signal. Brain homogenate from terminally sick mice infected with RML prion strain (either subjected to PMCA or not) was used as control.

Statistical Analysis

Mean values are presented with their standard errors of the mean (S.E.M.). Log-rank test was used for the survival and incubation time analysis. Unpaired *t* test, two tailed, was used for *p* calculation. Statistical analysis and graphic representations were performed with Prism software (5.0v GraphPad). Densitometric analysis was performed using ImageJ software (1.48v).

Results

Different Prion Isolates Are Generated In Vivo

We have previously generated a synthetic prion isolate that was challenged in wild-type outbred Crl:CD1(ICR) (CD-1) mice producing a severe disease phenotype [23]. A second passage transmission was then performed and 2 μL of brain homogenate was stereotaxically injected in the hippocampus of CD-1 animals ($n = 35$). All mice succumbed to the disease with 100% attack rate. Biochemical analysis of the CNS revealed that the 80% of the animals contained a PrP^{Sc} characterized by the prevalence of the monoglycosilated band (PrP^{Sc}-M), while the remaining 20% accumulated PrP^{Sc} with a prevalence of the diglycosylated band (PrP^{Sc}-D) (Fig. 1a). The animals with PrP^{Sc}-M had an incubation time of 130.90 ± 0.86 and a survival time of 164.66 ± 2.81 (mean ± S.E.M.) (Fig. 1b, black line), while the incubation and survival times of the animals with PrP^{Sc}-D were 162 ± 6.18 and 227.50 ± 6.33, respectively (mean ± S.E.M.) (Fig. 1b, red line). Thus, animals with PrP^{Sc}-M were characterized by shorter disease duration than animals with PrP^{Sc}-D. Finally, animals with PrP^{Sc}-D gained weight in the first stage of the disease which was then lost in the final stage, while animals with PrP^{Sc}-M showed a constant loss of weight (Fig. 1c). These results are summarized in Table 1.

Spleens and eyes of these animals were also analyzed to assess the tropism of both isolates for peripheral tissues. We have found PrP^{Sc} in the eyes of all the animals, which maintained the biochemical properties of those present in the brain. On the contrary, mice with PrP^{Sc}-D in the brain did not have PrP in the spleen, while mice with PrP^{Sc}-M had a strong PrP^{Sc} signal in the spleen but surprisingly the biochemical profile of this protein was different from that present in the brain. It was indeed characterized by a prevalence of the diglycosylated band (Fig. S1). However, PrP^{Sc}-M and PrP^{Sc}-D spleen-derived PrP^{Sc} were subjected to PMCA analysis and showed the amplification of diglycosylated PrP^{Sc} in both inocula (Fig. S2). These observations indicate that PrP present in our inoculum was able to adopt two alternative conformations associated with different disease phenotypes.

Newly Generated Prion Isolates Produced Different Neuropathological Alterations in Mice

Immunohistochemical analysis confirmed that PrP^{Sc}-M and PrP^{Sc}-D produced different neuropathological alterations in the brain of injected animals. In particular, after treatment with PK, samples were immunostained with anti-PrP antibody (6H4) and revealed that mice with PrP^{Sc}-M had a synaptic and widespread deposition of prion throughout the brain. On the contrary, mice with PrP^{Sc}-D showed prion deposition mainly confined to the *stratum lacunosum moleculare* of the hippocampus and to the deep layers of the cortex with the presence of few plaque-like deposits, which did not possess the tintorial properties of amyloid (Fig. 2a and Fig. S3). Glial activation was found to correlate with PrP^{Sc} deposition (either in terms of localization or in terms intensity of the signal), which was different between both groups of animals (Fig. 2a). Lesion profile was performed on hematoxylin and eosin-stained sections in nine brain areas clearly showed that PrP^{Sc}-M and PrP^{Sc}-D animals possess different topographic distributions of spongiform alterations [7]. In particular, the medulla and hippocampus are mostly affected in PrP^{Sc}-D animals, while the thalamus and cingulated cortex are mostly involved in PrP^{Sc}-M animals (Fig. 2b, c).

Newly Generated Prion Isolates Possess Different Biochemical and Biophysical Properties

To better characterize the biochemical and biophysical properties of PrP^{Sc}-M and PrP^{Sc}-D, we performed (i) PK resistance and (ii) conformational stability assays. The samples were then analyzed by means of Western blotting and densitometric analysis. The

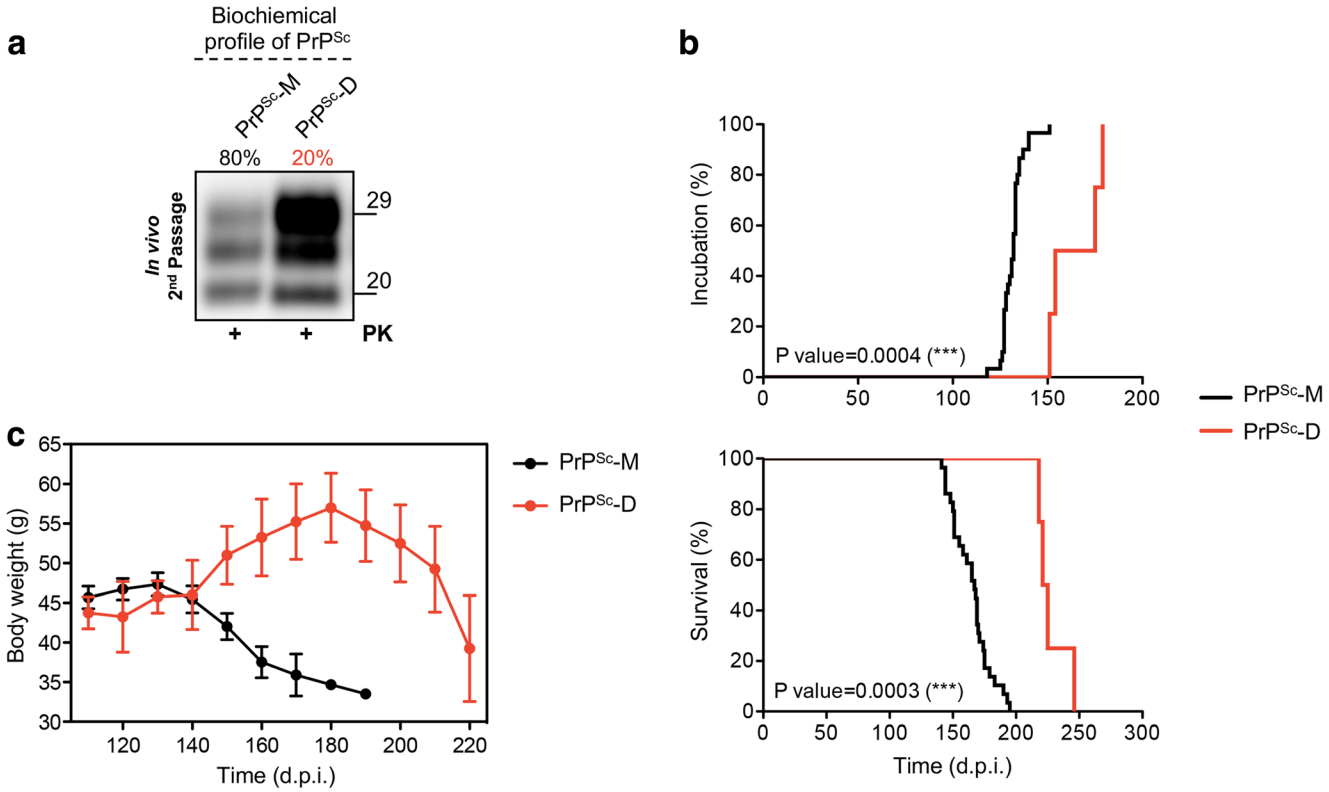

Fig. 1 In vivo generation of two newly prion isolates with distinct biochemical and clinical characteristics. **a** Western blot analysis of brain homogenates. The PrP^{Sc} signals were detected using 6D11 anti-PrP antibody. Two biochemical phenotypes of PrP^{Sc} were found among animals injected: 80% of animals displayed accumulation of PrP^{Sc} characterized by the prevalence of monoglycosylated isoform of PrP (PrP^{Sc}-M) while 20% of mice reveal accumulation of dyglicosylated PrP^{Sc} (PrP^{Sc}-D). **b** Incubation and survival time of mice with PrP^{Sc}-M and PrP^{Sc}-D. Statistical differences were found between the incubation time (IT) and survival time (ST) of PrP^{Sc}-M (IT 130.90 ± 0.86, ST 164.66 ± 2.81) and PrP^{Sc}-D (IT 162 ± 6.18, ST 227.50 ± 6.33) (mean ± S.E.M.). **c** Body weight assessment of animals with PrP^{Sc}-M and PrP^{Sc}-D. Animals with PrP^{Sc}-D showed body weight increasing in the first stage of the disease with a rapid decline only in the terminal stage. By contrast, animals with PrP^{Sc}-M displayed constant decreasing of body weight

results were plotted in a graph and revealed that PrP^{Sc}-D appeared to be more resistant to PK digestion than PrP^{Sc}-M (Fig. 3a). Conformational stability assay revealed that PrP^{Sc}-M is more stable against the GdnHCl treatment with respect to PrP^{Sc}-D. Especially, significant differences were observed at 3 M concentration of chaotropic agent (Fig. 3b). To sum up, as reported in Table 1, PrP^{Sc}-M is less resistant to PK digestion but more stable against guanidine treatment than PrP^{Sc}-D which is instead more resistant to PK but less stable in GdnHCl. We have finally determined the concentration of GdnHCl required to unfold half of PrP^{Sc} [$GdnHCl_{1/2}$]. As reported in the graph (Fig. 3c), we found statistically significant differences between the [$GdnHCl_{1/2}$] of PrP^{Sc}-M (3.344 ± 0.1663) and the [$GdnHCl_{1/2}$] of PrP^{Sc}-D (1.904 ± 0.2695) (mean (*M*) ± S.E.M.).

PMCA Analysis of Newly Generated Prion Isolates

PrP^{Sc}-M and PrP^{Sc}-D were analyzed by means of PMCA to assess their amplification's efficiency and their ability to retain the biochemical features of the original inoculum. Results confirmed that both isolates were able to efficiently amplify but, regardless of the inoculum (PrP^{Sc}-M or PrP^{Sc}-D), the final products of amplification were all characterized by a PrP^{Sc} with a prevalence of the diglycosylated band (Fig. 4a). PMCA experiments were serial dilutions of PrP^{Sc}-M and PrP^{Sc}-D (from 10^{-3} to the 10^{-12}) were subjected to two rounds of amplification confirmed that, regardless of the dilutions and the biochemical profile of the inocula, efficient amplification of PrP^{Sc} characterized by a predominance of the diglycosylated form of the

Table 1 Clinical features and biochemical characteristics of PrP^{Sc}-M and PrP^{Sc}-D

	Body weight	I.T.	S.T.	PK resistance	GdnHCl stability
PrP^{Sc}-M	Decreases	130.90 ± 0.86	164.66 ± 2.81	Low	High
PrP^{Sc}-D	Increases	162 ± 6.18	227.50 ± 6.33	High	Low

I.T and S.T. (days ± S.E.M.) ($n = 35$)

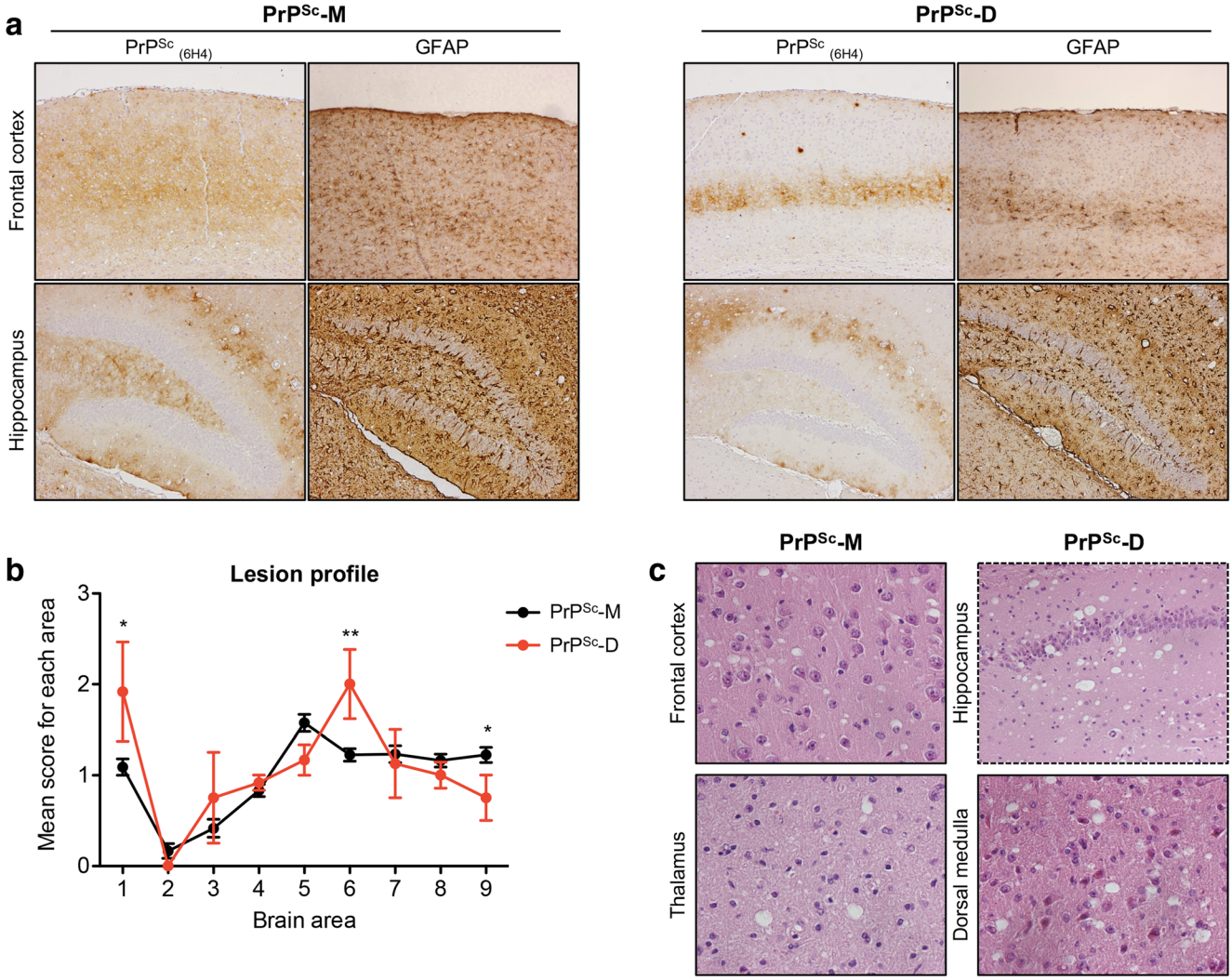

Fig. 2 Neuropathological characterization of newly generated prion isolates. **a** Neuropathological analysis of animals with PrP^{Sc}-M and PrP^{Sc}-D. Frontal cortex and hippocampus regions are shown. Animals with PrP^{Sc}-M were characterized by synaptic-diffused deposition of PrP^{Sc} while animals with PrP^{Sc}-D showed PrP immunoreactivity mainly confined in deep layers of the cortex and stratum lacunosum moleculare of the hippocampus. GFAP immunoreactivity correlate with PrP^{Sc} deposition differences between PrP^{Sc}-M and PrP^{Sc}-D. **b** Lesion profile of animals with PrP^{Sc}-M and PrP^{Sc}-D. Spongiform changes were evaluated and scored on hematoxylin and eosin-stained sections in nine brain areas: (1) dorsal medulla, (2) cerebellar cortex, (3) superior culliculus, (4) hypothalamus,(5) thalamus, (6) hippocampus, (7) septum, (8) retrosplenial and adjacent motor cortex, and (9) cingulated and adjacent motor cortex. Animals with PrP^{Sc}-M were mainly characterized by lesions in the thalamus and frontal cortex while the hippocampus and dorsa medulla appeared most affected in animals with PrP^{Sc}-D. ($*p < 0.05$, $**p < 0.01$). **c** Hematoxylin and eosin-stained sections of the most affected brain areas

protein was observed (Fig. S4). This result indicates that the biochemical profile of PrP^{Sc}-D was maintained while that of PrP^{Sc}-M was lost during the amplification process and new biochemical features were acquired. To have a better understanding of these data, we tested the fidelity of PMCA amplification by subjecting mouse adapted vCJD (MoPrP-vCJD) and RML prion strains to several rounds of PMCA. MoPrP-vCJD is indeed characterized by the presence of PrP^{Sc}-D, while RML shows PrP^{Sc}-M. After amplification, the biochemical characteristics of both prion strains were retained, thus suggesting that PMCA is able to amplify different prion strains with high fidelity. For this reason, the amplification products of PrP^{Sc}-M suggest that a process of adaptation or selection might have occurred and gave rise to the formation of an isolate with different biochemical features.

Biochemical and Biophysical Analysis of the Final PMCA Product and Comparison with the Original Isolates

Final PMCA products (either from PrP^{Sc}-M or from PrP^{Sc}-D) were subjected to biochemical and biophysical analysis, including (i) PK resistance assay (Fig. 4b) and (ii) conformational stability assay with GdnHCl (Fig. 4c). All the samples showed similar resistance to PK digestion and stability in the presence of GdnHCl, supporting the fact that, regardless of the inoculum

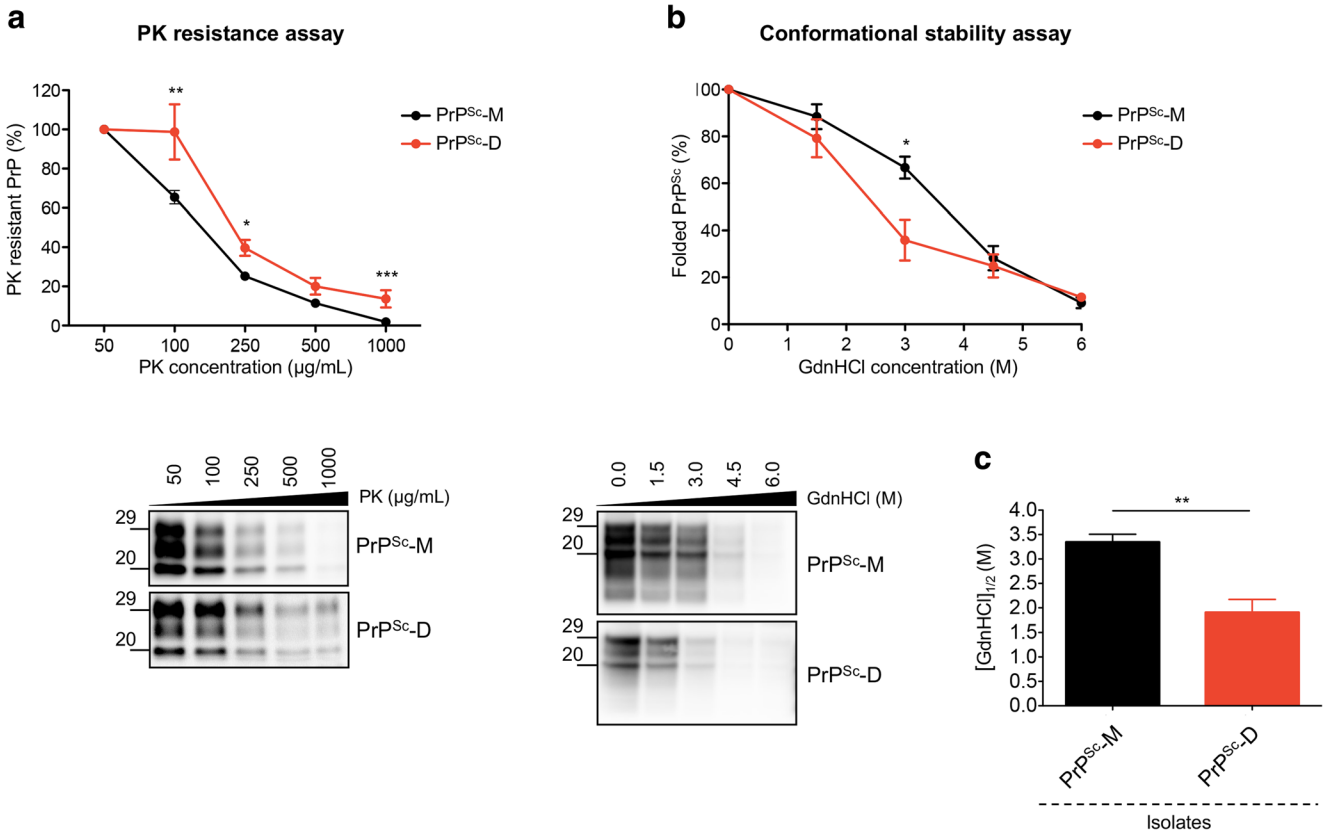

Fig. 3 Biophysical assessment of newly generated isolates. **a** PK resistance assay. PrP^{Sc}-D isolates were characterized by high resistance against proteolytic treatment if compared to PrP^{Sc}-M isolates, especially at 100, 250 and 1000 μg/mL of PK concentration where the difference reached statistical significance (*$p < 0.05$, **$p < 0.01$, ***$p < 0.001$). **b** Conformational stability assay. PrP^{Sc}-M isolates shown higher resistance to chaotropic treatment respect to that of PrP^{Sc}-D isolates. At 3 M concentration of GdnHCl were founded statistical differences between PrP^{Sc}-M and PrP^{Sc}-D (*$p < 0.05$). **c** $[GdnHCl]_{1/2}$ of PrP^{Sc}-M and PrP^{Sc}-D isolates. After nonlinear regression (Boltzmann sigmoidal), the concentrations required to unfold half of PrP^{Sc} were calculated with GraphPad software. Significant differences (**$p < 0.01$) were observed between PrP^{Sc}-M and PrP^{Sc}-D characterized by a $[GndHCl]_{1/2}$ of 3.344 ± 0.166 and 1.904 ± 0.269 (GdnHCl (M) ± S.E.M.) respectively

(PrP^Sc-M or PrP^Sc-D), PMCA was able to generate a unique isolate, termed PrP^Sc-PMCA. This isolate was characterized by the presence of a PrP^Sc with a predominance of the diglycosylated band. Since this biochemical profile is similar to that of PrP^Sc-D, we wondered whether PMCA might have indeed preferentially amplified PrP^Sc-D, thus demonstrating that it might coexist with PrP^Sc-M. Surprisingly, PK resistance and GdnHCl assays showed that PrP^Sc-PMCA possessed biophysical features quite different from those of either PrP^Sc-M or PrP^Sc-D. In particular, PrP^Sc-PMCA was much more resistant to PK and more stable in GdnHCl than PrP^Sc-M and PrP^Sc-D (Fig. 4b, c). These data show that PMCA generated a third prion isolate.

RT-QuIC Analysis of In Vivo (PrP^Sc-D and PrP^Sc-M) and In Vitro (PrP^Sc-PMCA) Generated Isolates

PrP^Sc-M, PrP^Sc-D, and PrP^Sc-PMCA were finally analyzed by means of RT-QuIC to assess whether these isolates were characterized by different seeding activities. All the isolates possessed seeding activity of mouse recombinant PrP (23–230), which was efficiently triggered by all of them, without significant differences in terms of kinetic of aggregation and fluorescence intensity (Fig. S5A). By further analyzing the slope that numerically describes the steepness of the kinetic curves, we have found that the slope of PrP^Sc-M was smaller than that of PrP^Sc-D (Fig. S5B), thus further sustaining the fact that both isolates are different from each other. The slope of PrP^Sc-PMCA acquired an intermediate value between PrP^Sc-M and PrP^Sc-D but still statistically different from either of them. These findings suggested that also PrP^Sc-PMCA seems to be a different strain characterized by its own seeding activity. As control, we analyzed the seeding activity of RML brain homogenate either before or after PMCA amplification. In this case, the slopes of the curves were similar and not statistically significant differences were found, thus confirming that, likely, PMCA amplified this strain with high fidelity (Fig. S5C).

Discussion

We have previously shown the in vivo infectious properties of a synthetic prion amyloid prepared using recombinant full-

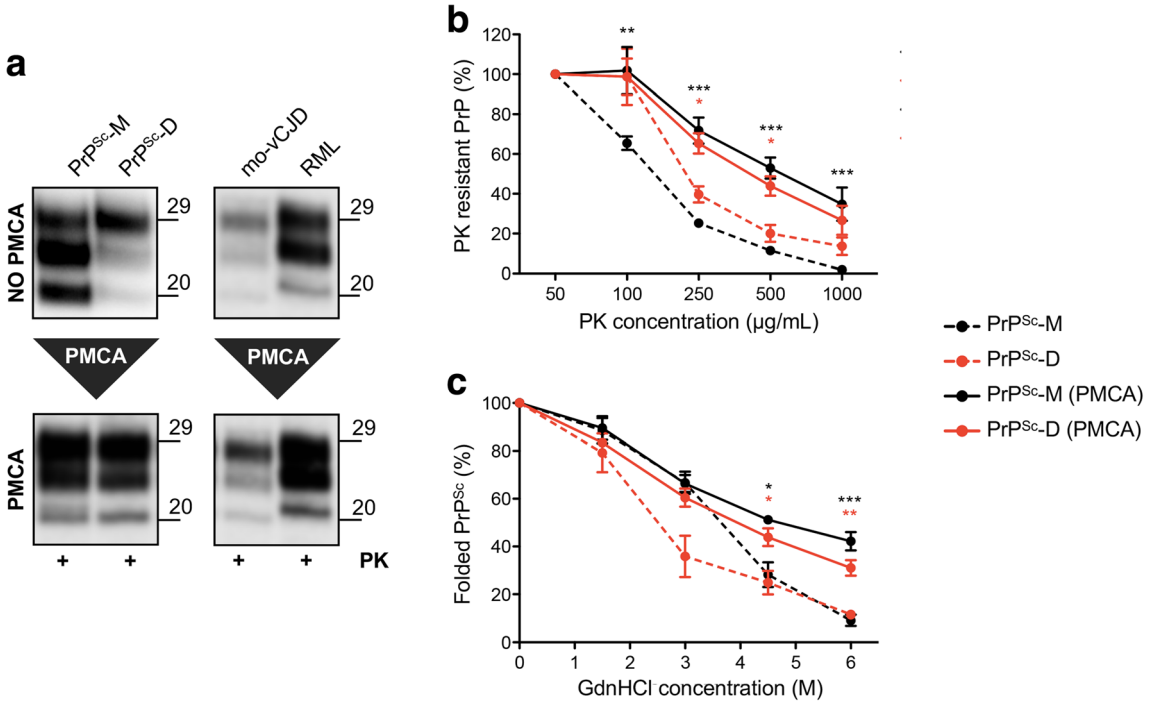

Fig. 4 PMCA amplification and biophysical characterization of newly generated isolates. **a** PMCA analysis of PrP^{Sc}-M and PrP^{Sc}-D isolates and comparison with RML and mouse adapted variant CJD (mo-vCJD) prion strains. PrP^{Sc}-M and PrP^{Sc}-D were amplified by means of PMCA along with RML and mo-vCJD that were used as control to monitor the fidelity of the amplification. Surprisingly, after PMCA, all the amplified products were characterized by a prevalence of the dyglicosylated isoform of PrP^{Sc}. By contrast, RML and mo-vCJD maintain their biochemical features after the amplification. **b** PK resistance assay of the amplified products. Compared to PrP^{Sc}-M and PrP^{Sc}-D, PMCA amplified product possessed significantly higher resistance to PK digestion at all concentrations of enzyme tested (*$p < 0.05$, **$p < 0.01$, ***$p < 0.001$). **c** Conformational stability assay. The densitometric analysis was reported in the plot as % of folded PrP^{Sc} after the GdnHCl treatment. PMCA amplified products possess higher conformational stability profile that differ from that we observed in vivo either for PrP^{Sc}-M or for PrP^{Sc}-D isolates especially at 4.5 and 6 M concentrations of GdnHCl (*$p < 0.05$, **$p < 0.01$, ***$p < 0.001$)

length mouse PrP and subsequently misfolded under controlled biophysical and biochemical conditions [23]. Particularly, after amplification by means of PMCA, this isolate was injected in mice and produced a PrP^{Sc} with novel strain-specified properties. In the present study, we analyzed the effect of this isolate when challenged in a second in vivo passage using wild-type CD-1 mice. All the animals succumbed to prion disease but in their brains, we could detect the presence of two different prions. In the 80% of the cases, the protein was characterized by a predominance of the monoglycosylated band (PrP^{Sc}-M), while in the other 20%, it was characterized by a predominance of the diglycosylated isoform (PrP^{Sc}-D). These differences in the biochemical profiles were associated to different (i) clinical manifestations of the disease (including incubation time, survival time, and body weight fluctuations), (ii) neuropathological changes (deposition of PrP^{Sc} and spongiform alterations), (iii) biochemical and biophysical features of both PrP^{Sc} (PK resistance assay and GdnHCl conformational stability assays), and different seeding activities when assessed by means of RT-QuIC. In particular, PrP^{Sc}-M induces a faster disease progression, was less resistant to PK digestion, and showed a higher stability to GdnHCl denaturation compared to PrP^{Sc}-D. Higher resistance to PK digestion and lower stability in the presence of GdnHCl than PrP^{Sc}-M instead characterized the latter, which induced slower disease progression. Considering data from the literature, the conformational stability of prion strains appear closely related to the clinical course of the disease [34]. For instance, as reported for hyper (HY) and drowsy (DY) in hamsters, PrP^{Sc} associated to HY is characterized by high conformational stability and induces faster disease progression while that associated to DY possesses low conformational stability and is responsible for longer disease duration. This correlation was also found in our synthetic prion isolates, where PrP^{Sc}-M is more stable and it induced shorter disease duration than PrP^{Sc}-D, which in turn is less stable and leads to longer disease duration. As reported by previous studies [34–36], the inverse relationship between PrP^{Sc} stability and disease duration cannot be assumed as general model, particularly in the case of synthetically derived prion strains. Recent data [37] suggests that this characteristic might be influenced by (i) recPrP primary sequence of synthetic prions and (ii) the animal model used for bioassays.

Finally, RT-QuIC experiments showed that both isolates possessed different seeding activities. Altogether, these data support the hypothesis that the in vivo

bioassay was able to generate two different isolates that spontaneously arose from our original inoculum due to mechanisms of selection or adaptation that are not understood yet. It seems that the context of prion replication plays an important role in guiding these phenomena.

These insights suggest the intrinsically heterogeneous composition of prion strains and their ability to adapt in response to environment pressure in agreement to the Darwinian evolution theory [32]. Two main hypotheses were proposed as possible mechanism: the "cloud" hypothesis and the adaptation mechanism. The cloud hypothesis infers that the prion population is composed of a multitude of conformational variants. Changing the replication environment allows the most efficiently replicating variant to become the predominant component of the population which then constitutes a distinct sub-strain [32]. On the contrary, the adaptation mechanism consists of a long clinically silent stage which is accompanied by a slow modification of the biophysical and neuropathological properties of PrP^{Sc}. The long adaptation period of synthetic prion when injected in animals is attributed to structural changes of PrP conformation that, in a mechanism named "deformed templating," lead to a generation of an authentic PrP^{Sc}. The deformed templating mechanism proposed that the first product of PrP^{C} misfolding triggered by recombinant amyloids generate a self-replicating state of PrP named atypical PrP^{Sc}. After several serial passages, the atypical PrP^{Sc} gave rise to a PrP^{Sc} with specific biochemical and neuropathological characteristics [38, 39].

When analyzing the spleen of PrP^{Sc}-M animals, we found high accumulation of PrP^{Sc} whose biochemical profile was characterized by the prevalence of diglycosylated band. These differences might be due to different environments of replication (CNS vs spleen) that might have selected the best isolate to replicate in that context. The presence of different types of cells between CNS and spleen, cellular metabolism, and connections with other tissues and fluids might have a role in this selection process.

We are not able to determine whether the generation of two isolates is mainly due to either a process of selection or a process of adaptation. Indeed, the original inoculum, although produced using highly pure source of recombinant PrP and strictly controlled biochemical conditions, might have produced different isolates of misfolded PrP. When passaged in mice, only two of these isolates seemed to replicate with higher efficiency compared to others, which induced different pathologies. It is reasonable to argue that, although not detectable, the other isolates might still be present and able to replicate with lower efficiency. The amplification of the two isolates might have also been favored by the characteristics of the outbred animals utilized in the in vivo experiments. Recent evidence shows that minimal variations in the genetic background of the host animals can significantly influence the biochemical features of PrP^{Sc} [40]. Therefore, differences in the genetic background of CD-1 animals might have favored the replication of PrP^{Sc}-M or PrP^{Sc}-D while interfering with the replication of other isolates. However, differences in the level of PrP^{C} expression were shown to play a role in driving the glycosylation pattern of PrP^{Sc} [41]. Considering that PrP^{Sc}-M and PrP^{Sc}-D differentially accumulated in distinct brain regions, we might speculate that such areas might be characterized by the presence of slightly different levels of PrP^{C} that can significantly influence the glycosylation of our isolates. Finally, the ubiquitin-proteasome system (UPS) and lysosomal system may contribute to the prevalent selection of some prion isolates and not others [22, 42–44].

Compelling evidence suggests that prions can change their abnormal conformation in response to spontaneous events unrelated to changes of the environment of replication [45]. These phenomena might also explain the appearance of new prion strains after inter-species prion transmission. In this scenario, the pressure exerted either by the new environment or by the differences in PrP^{C} sequence might force the protein to misfold with different conformations.

As observed for natural-derived prion strains, also, synthetic prion strains may undergo a process of adaptation after animal passages [20–22]. Hamster synthetic SSLOW strain required four serial passages in wild-type Syrian hamsters before being stabilized and able to induce reproducible neuropathological alterations. The effects of strain selection and adaptation seem not to occur in the case of well-adapted prion strains like classical RML, where no differences were reported after its inoculation in different strains of animals (either genetically modified or wild-type). Differently to RML, our original inoculum was not cloned throughout several passages in mice; thus, it might be exposed to a strong process of selection due to several factors described above. These data show that either the environment or other factors contribute to (1) altering the conformation of PrP giving rise to new ones whose replication is more efficient in the modified environment or (2) favoring the replication of few prion isolates over others that might coexist in the same strain.

Through PMCA analysis, which is able to mimic the process of in vivo prion replication, we further assessed the ability of both PrP^{Sc}-M and PrP^{Sc}-D to adapt their conformations by changing the replication environment. Surprisingly, after one round of amplification, both PrP^{Sc}-M and PrP^{Sc}-D gave rise to a different amplified product (PrP^{Sc}-PMCA), which was not found in vivo. The latter, although bearing the same biochemical profile of PrP^{Sc}-D, possessed biophysical properties that were quite different from those of PrP^{Sc}-M and PrP^{Sc}-D. We do not know the precise mechanisms involved in this selection but a fundamental aspect that we need to consider is that PMCA provides solely the permissive environment for prion replication, without the presence of any cellular mechanisms like proteolysis (the substrates were prepared in buffers containing protease inhibitors) and acidic pH compartments. Acidic pH of endosomal compartments has been suggested as relevant for PrP^{C}/PrP^{Sc} conversion [46], while the pH of the PMCA reaction is neutral, homogenous, and stable. Thus, the replication of a third isolate might have prevailed over

the others. Indeed, PMCA exposes the samples to high-power cyclical sonication and can contribute in changing the biochemical and biophysical features of the final amplified product. The PMCA amplified isolates are likely to be infectious since data from the literature indicate the ability of PMCA to produce bona fide prions able to retain their biological and infectious features when injected in animals [47–50].

Likely, the context of PMCA amplification can impose an *evolutionary* pressure that may select the isolate able to better replicate in this environment. Therefore, we can infer that the PrP^{Sc} conformation amplified by PMCA might have been present in all the animal brains but was not able to replicate in vivo. Recent data show that recombinant prions can be selected by changing polyanionic cofactors in the substrate of PMCA [51]. The presence of cofactors is not necessary for in vitro prion propagation but appeared involved in the selection of specific sub-strains. In conclusion, our data indicate that prion selection and adaptation are phenomena that may occur in response to changes in the context of replication. Events of prion selection were already observed after pharmacological treatment of cell cultures [32] or infected animals [52, 53] where the generation of drug-resistant variants of the original PrP strain were described. This is because the pharmacological treatments were able to modify the environment, thus inhibiting the replication of specific strains while selecting drug-resistant conformations that can replicate in the new environment and sustain the pathological process. This might explain why there are still no effective therapies for these devastating disorders. The possibility to modulate the replication environment by exploiting innovative techniques such as PMCA and RT-QuIC would help to an understanding of the mechanism of prion selection and adaptation in response to cellular environmental changes and identify novel pharmacological target for anti-prion compound.

Acknowledgements The authors wish to thank Associazione Italiana Encefalopatie da Prioni (A.I.En.P.).

Authors Contributions EB, FM, and GL designed the experiments and EB, TV, IC, CMGDL, MR, and GS performed the practical work. TV and IC performed the animal inoculations. EB, FM, GG, FT, and GL wrote and revised the manuscript. All the authors read and approved the final manuscript.

Funding This work was supported/partially supported by the Italian Ministry of Health (GR-2013-02355724 and RC) to FM, the Italian Ministry of Health to FT, and the International School for Advanced Studies (SISSA) intramural funding to GL.

Compliance with Ethical Standards

The study, including its Ethics aspects, was approved by the Italian Ministry of Health (Permit Number, NP-02-14).

Conflict of Interest The authors declare that there are no conflicts of interest.

References

1. McKinley MP, Bolton DC, Prusiner SB (1983) A protease-resistant protein is a structural component of the scrapie prion. Cell 35(1): 57–62
2. Tanaka M, Chien P, Naber N, Cooke R, Weissman JS (2004) Conformational variations in an infectious protein determine prion strain differences. Nature 428(6980):323–328
3. Bartz JC (2016) Prion strain diversity. Cold Spring Harb Perspect Med 6(12)
4. Dickinson AG, Meikle VM (1971) Host-genotype and agent effects in scrapie incubation: change in allelic interaction with different strains of agent. Mol Gen Genet 112(1):73–79
5. Carp RI, Callahan SM, Sersen EA, Moretz RC (1984) Preclinical changes in weight of scrapie-infected mice as a function of scrapie agent-mouse strain combination. Intervirology 21(2):61–69
6. Fraser H (1993) Diversity in the neuropathology of scrapie-like diseases in animals. Br Med Bull 49(4):792–809
7. Fraser H, Dickinson AG (1968) The sequential development of the brain lesion of scrapie in three strains of mice. J Comp Pathol 78(3): 301–311
8. Khalili-Shirazi A, Summers L, Linehan J, Mallinson G, Anstee D, Hawke S, Jackson GS, Collinge J (2005) PrP glycoforms are associated in a strain-specific ratio in native PrPSc. J Gen Virol 86(Pt 9): 2635–2644
9. Peretz D, Williamson RA, Legname G, Matsunaga Y, Vergara J, Burton DR, DeArmond SJ, Prusiner SB et al (2002) A change in the conformation of prions accompanies the emergence of a new prion strain. Neuron 34(6):921–932
10. Safar J, Wille H, Itri V, Groth D, Serban H, Torchia M, Cohen FE, Prusiner SB (1998) Eight prion strains have PrP(Sc) molecules with different conformations. Nat Med 4(10):1157–1165
11. Caughey B, Raymond GJ, Bessen RA (1998) Strain-dependent differences in beta-sheet conformations of abnormal prion protein. J Biol Chem 273(48):32230–32235
12. Makarava N, Savtchenko R, Baskakov IV (2013) Selective amplification of classical and atypical prions using modified protein misfolding cyclic amplification. J Biol Chem 288(1):33–41
13. Morales R, Abid K, Soto C (2007) The prion strain phenomenon: molecular basis and unprecedented features. Biochim Biophys Acta 1772(6):681–691
14. Bartz JC, Bessen RA, McKenzie D, Marsh RF, Aiken JM (2000) Adaptation and selection of prion protein strain conformations following interspecies transmission of transmissible mink encephalopathy. J Virol 74(12):5542–5547
15. Bessen RA, Marsh RF (1992) Identification of two biologically distinct strains of transmissible mink encephalopathy in hamsters. J Gen Virol 73(Pt 2):329–334
16. Bessen RA, Marsh RF (1994) Distinct PrP properties suggest the molecular basis of strain variation in transmissible mink encephalopathy. J Virol 68(12):7859–7868
17. Bessen RA, Marsh RF (1992) Biochemical and physical properties of the prion protein from two strains of the transmissible mink encephalopathy agent. J Virol 66(4):2096–2101
18. Legname G, Baskakov IV, Nguyen HO, Riesner D, Cohen FE, DeArmond SJ, Prusiner SB (2004) Synthetic mammalian prions. Science 305(5684):673–676
19. Colby DW, Giles K, Legname G, Wille H, Baskakov IV, DeArmond SJ, Prusiner SB (2009) Design and construction of diverse mammalian prion strains. Proc Natl Acad Sci U S A 106(48):20417–20422
20. Jeffrey M, McGovern G, Makarava N, Gonzalez L, Kim YS, Rohwer RG, Baskakov IV (2014) Pathology of SSLOW, a transmissible and fatal synthetic prion protein disorder, and comparison

with naturally occurring classical transmissible spongiform encephalopathies. Neuropathol Appl Neurobiol 40(3):296–310
21. Makarava N, Kovacs GG, Savtchenko R, Alexeeva I, Budka H, Rohwer RG, Baskakov IV (2012) Stabilization of a prion strain of synthetic origin requires multiple serial passages. J Biol Chem 287(36):30205–30214
22. Makarava N, Kovacs GG, Bocharova O, Savtchenko R, Alexeeva I, Budka H, Rohwer RG, Baskakov IV (2010) Recombinant prion protein induces a new transmissible prion disease in wild-type animals. Acta Neuropathol 119(2):177–187
23. Moda F, Le TN, Aulic S, Bistaffa E, Campagnani I, Virgilio T, Indaco A, Palamara L et al (2015) Synthetic prions with novel strain-specified properties. PLoS Pathog 11(12):e1005354
24. Saborio GP, Permanne B, Soto C (2001) Sensitive detection of pathological prion protein by cyclic amplification of protein misfolding. Nature 411(6839):810–813
25. Saa P, Castilla J, Soto C (2006) Ultra-efficient replication of infectious prions by automated protein misfolding cyclic amplification. J Biol Chem 281(46):35245–35252
26. Bieschke J, Weber P, Sarafoff N, Beekes M, Giese A, Kretzschmar H (2004) Autocatalytic self-propagation of misfolded prion protein. Proc Natl Acad Sci U S A 101(33):12207–12211
27. Atarashi R, Wilham JM, Christensen L, Hughson AG, Moore RA, Johnson LM, Onwubiko HA, Priola SA et al (2008) Simplified ultrasensitive prion detection by recombinant PrP conversion with shaking. Nat Methods 5(3):211–212
28. Castilla J, Gonzalez-Romero D, Saa P, Morales R, De Castro J, Soto C (2008) Crossing the species barrier by PrP(Sc) replication in vitro generates unique infectious prions. Cell 134(5):757–768
29. Barria MA, Telling GC, Gambetti P, Mastrianni JA, Soto C (2011) Generation of a new form of human PrP(Sc) in vitro by interspecies transmission from cervid prions. J Biol Chem 286(9):7490–7495
30. Chianini F, Fernandez-Borges N, Vidal E, Gibbard L, Pintado B, de Castro J, Priola SA, Hamilton S et al (2012) Rabbits are not resistant to prion infection. Proc Natl Acad Sci U S A 109(13):5080–5085
31. Gonzalez-Montalban N, Lee YJ, Makarava N, Savtchenko R, Baskakov IV (2013) Changes in prion replication environment cause prion strain mutation. FASEB journal : official publication of the Federation of American Societies for Experimental Biology 27(9):3702–3710
32. Mahal SP, Browning S, Li J, Suponitsky-Kroyter I, Weissmann C (2010) Transfer of a prion strain to different hosts leads to emergence of strain variants. Proc Natl Acad Sci U S A 107(52):22653–22658
33. Vascellari S, Orru CD, Hughson AG, King D, Barron R, Wilham JM, Baron GS, Race B et al (2012) Prion seeding activities of mouse scrapie strains with divergent PrPSc protease sensitivities and amyloid plaque content using RT-QuIC and eQuIC. PLoS One 7(11):e48969
34. Ayers JI, Schutt CR, Shikiya RA, Aguzzi A, Kincaid AE, Bartz JC (2011) The strain-encoded relationship between PrP replication, stability and processing in neurons is predictive of the incubation period of disease. PLoS Pathog 7(3):e1001317
35. Bett C, Joshi-Barr S, Lucero M, Trejo M, Liberski P, Kelly JW, Masliah E, Sigurdson CJ (2012) Biochemical properties of highly neuroinvasive prion strains. PLoS Pathog 8(2):e1002522
36. Legname G, Nguyen HO, Peretz D, Cohen FE, DeArmond SJ, Prusiner SB (2006) Continuum of prion protein structures enciphers a multitude of prion isolate-specified phenotypes. Proc Natl Acad Sci U S A 103(50):19105–19110
37. Hannaoui S, Amidian S, Cheng YC, Duque Velasquez C, Dorosh L, Law S, Telling G, Stepanova M et al (2017) Destabilizing polymorphism in cervid prion protein hydrophobic core determines prion conformation and conversion efficiency. PLoS Pathog 13(8):e1006553
38. Makarava N, Baskakov IV (2012) Genesis of tramsmissible protein states via deformed templating. Prion 6(3):252–255
39. Makarava N, Kovacs GG, Savtchenko R, Alexeeva I, Ostapchenko VG, Budka H, Rohwer RG, Baskakov IV (2012) A new mechanism for transmissible prion diseases. J Neurosci 32(21):7345–7355
40. Lloyd SE, Linehan JM, Desbruslais M, Joiner S, Buckell J, Brandner S, Wadsworth JD, Collinge J (2004) Characterization of two distinct prion strains derived from bovine spongiform encephalopathy transmissions to inbred mice. J Gen Virol 85(Pt 8):2471–2478
41. Le Dur A, Lai TL, Stinnakre MG, Laisne A, Chenais N, Rakotobe S, Passet B, Reine F et al (2017) Divergent prion strain evolution driven by PrP(C) expression level in transgenic mice. Nat Commun 8:14170
42. Bueler H, Aguzzi A, Sailer A, Greiner RA, Autenried P, Aguet M, Weissmann C (1993) Mice devoid of PrP are resistant to scrapie. Cell 73(7):1339–1347
43. Goold R, McKinnon C, Tabrizi SJ (2015) Prion degradation pathways: potential for therapeutic intervention. Mol Cell Neurosci 66(Pt A):12–20
44. McKinnon C, Goold R, Andre R, Devoy A, Ortega Z, Moonga J, Linehan JM, Brandner S et al (2016) Prion-mediated neurodegeneration is associated with early impairment of the ubiquitin-proteasome system. Acta Neuropathol 131(3):411–425
45. Weissmann C, Li J, Mahal SP, Browning S (2011) Prions on the move. EMBO Rep 12(11):1109–1117
46. Yim YI, Park BC, Yadavalli R, Zhao X, Eisenberg E, Greene LE (2015) The multivesicular body is the major internal site of prion conversion. J Cell Sci 128(7):1434–1443
47. Gonzalez-Montalban N, Makarava N, Ostapchenko VG, Savtchenk R, Alexeeva I, Rohwer RG, Baskakov IV (2011) Highly efficient protein misfolding cyclic amplification. PLoS Pathog 7(2):e1001277
48. Moudjou M, Sibille P, Fichet G, Reine F, Chapuis J, Herzog L, Jaumain E, Laferriere F et al (2013) Highly infectious prions generated by a single round of microplate-based protein misfolding cyclic amplification. MBio 5(1):e00829–e00813
49. Shikiya RA, Bartz JC (2011) In vitro generation of high-titer prions. J Virol 85(24):13439–13442
50. Castilla J, Saa P, Hetz C, Soto C (2005) In vitro generation of infectious scrapie prions. Cell 121(2):195–206
51. Fernandez-Borges N, Di Bari MA, Erana H, Sanchez-Martin M, Pirisinu L, Parra B, Elezgarai SR, Vanni I et al (2017) Cofactors influence the biological properties of infectious recombinant prions. Acta Neuropathol
52. Ghaemmaghami S, Ahn M, Lessard P, Giles K, Legname G, DeArmond SJ, Prusiner SB (2009) Continuous quinacrine treatment results in the formation of drug-resistant prions. PLoS Pathog 5(11):e1000673
53. Bian J, Kang HE, Telling GC (2014) Quinacrine promotes replication and conformational mutation of chronic wasting disease prions. Proc Natl Acad Sci U S A 111(16):6028–6033